Lack of Enantioselectivity in the SULT1A3-catalyzed Sulfoconjugation of Normetanephrine Enantiomers: An *In Vitro* and Computational Study

ERIC GROUZMANN,[1]* JEAN-BAPTISTE GUALTIEROTTI,[2] SANDRINE GERBER-LEMAIRE,[2] KARIM ABID,[1] NOUREDDINE BRAKCH,[3] ALESSANDRO PEDRETTI,[4] BERNARD TESTA,[5] AND GIULIO VISTOLI[4]

[1]*Service de Biomédecine, Lausanne University Hospital (CHUV), Lausanne, Switzerland*
[2]*Ecole Polytechnique Fédérale de Lausanne, ISIC, LSPN, Batochime, Lausanne, Switzerland*
[3]*Department of Internal Medicine, Service of Nephrology, Lausanne University Hospital (CHUV), Lausanne, Switzerland*
[4]*Dipartimento di Scienze Farmaceutiche "Pietro Pratesi", Facoltà di Farmacia, Università degli Studi di Milano, Milano, Italy*
[5]*Department of Pharmacy, Lausanne University Hospital (CHUV), Lausanne, Switzerland*

ABSTRACT (1*R*)-Normetanephrine is the natural stereoisomeric substrate for sulfotransferase 1A3 (SULT1A3)-catalyzed sulfonation. Nothing appears known on the enantioselectivity of the reaction despite its potential significance in the metabolism of adrenergic amines and in clinical biochemistry. We confronted the kinetic parameters of the sulfoconjugation of synthetic (1*R*)-normetanephrine and (1*S*)-normetanephrine by recombinant human SULT1A3 to a docking model of each normetanephrine enantiomer with SULT1A3 and the 3′-phosphoadenosine-5′-phosphosulfate cofactor on the basis of molecular modeling and molecular dynamics simulations of the stability of the complexes. The K_M, V_{max}, and k_{cat} values for the sulfonation of (1*R*)-normetanephrine, (1*S*)-normetanephrine, and racemic normetanephrine were similar. *In silico* models were consistent with these findings as they showed that the binding modes of the two enantiomers were almost identical. In conclusion, SULT1A3 is not substrate-enantioselective toward normetanephrine, an unexpected finding explainable by a mutual adaptability between the ligands and SULT1A3 through an "induced-fit model" in the catalytic pocket. *Chirality, 00:000-000, 2012.*

KEY WORDS: sulfotransferase 1A3; normetanephrine; enantioselectivity; *in silico* models; enzyme kinetics; induced-fit model

INTRODUCTION

The physiological effects of norepinephrine and epinephrine are terminated by various conjugation pathways, notably 3-*O*-methoxylation to produce normetanephrine and metanephrine followed by sulfonation at the *para*-hydroxyl group (Fig. 1).[1] Among the 13 known human cytosolic sulfotransferases, sulfotransferase 1A3 (SULT1A3) (EC 2.8.2.1) is the enzyme that catalyzes the transfer of a sulfonyl group from the cofactor 3′-phosphoadenosine-5′-phosphosulfate (PAPS) to the free remaining *para*-hydroxyl group on the phenyl ring of metanephrine and normetanephrine.[2]

(1*R*)-Normetanephrine present in food or produced by our body is sulfonated during enterohepatic cycling by SULT1A3 located in the gastrointestinal tract.[3] Importantly, in the context of this study, normetanephrine is used as an important biomarker in the diagnosis and monitoring of patients suffering from pheochromocytoma/paraganglioma, which are tumors that secrete excessive amounts of catecholamines and free metanephrines.[4] In such bioanalyses, sulfoconjugated normetanephrine must first be hydrolyzed. The sole commercially available source of authentic sulfoconjugated normetanephrine is the racemate, which is normally used for calibration and quality control.[5] However, this is a potential source of problems because measurements involve an acid-catalyzed or enzymatic hydrolysis step to hydrolyze the sulfoconjugate to the free metabolite prior to analytical measurement by HPLC with electrochemical detection. For these reasons, we considered it significant to determine the substrate enantioselectivity of the sulfonation of normetanephrine enantiomers by SULT1A3 and find out whether their substitution by the racemic sulfated calibrator we previously described does or does not influence the results.[5]

There are indeed several reports on the substrate enantioselectivity of SULT1A3, which for example shows a unique sulfoconjugating activity toward (2*S*)-tyrosine and (2*S*)-(3′,4′-dihydroxyphenyl)alanine (L-DOPA), with a high enantioselectivity for their non-physiological (2*R*)-enantiomers.[6] The important role of Glu146 in the substrate specificity of SULT1A3 was demonstrated,[7,8] and the crystal structure of SULT1A3–PAPS–ligand complexes confirmed that residues Glu146 and Asp86 are crucial to the L-DOPA/tyrosine-sulfonating activity of SULT1A3 and play also a role in the stereoselectivity of the reaction.[6–8] There is also strong evidence that the sulfonation of β-adrenoceptor agonists and antagonists is enantioselective.[9–14] Extrapolating from the existing literature, we therefore expected the sulfoconjugation of synthetic (1*R*)-normetanephrine and (1*S*)-normetanephrine to be notably enantioselective and used recombinant human SULT1A3 to challenge this hypothesis. Experimental investigations were carried out to determine the enzymatic kinetic constants for each enantiomer of normetanephrine. The results were compared with computational models obtained by molecular modeling

Additional Supporting Information may be found in the online version of this article.

*Correspondence to: Eric Grouzmann, Service de Biomédecine, Lausanne University Hospital (CHUV), Avenue de Beaumont 29, CH-1011 Lausanne, Switzerland. E-mail: Eric.Grouzmann@chuv.ch

Received for publication 11 June 2012; Accepted 24 July 2012
DOI: 10.1002/chir.22108
Published online in Wiley Online Library (wileyonlinelibrary.com).

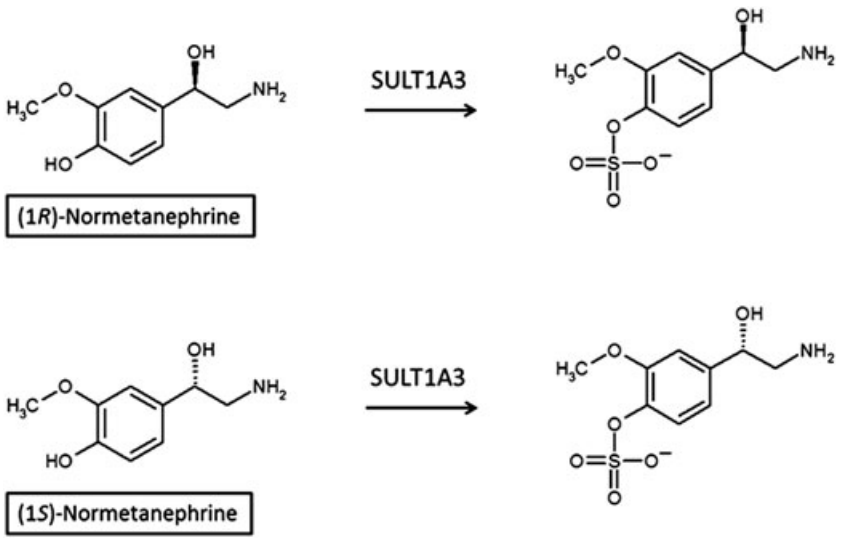

Fig. 1. The SULT1A3-catalyzed reaction whose substrate enantioselectivity is investigated here.

(MM) and molecular dynamics (MD) to explain the observed (and unexpected) lack of enantioselectivity of the reaction.

MATERIAL AND METHODS

Chemicals and Reagents

Racemic normetanephrine (rac-normetanephrine) was purchased from Sigma-Aldrich (St. Louis, Mo, USA). PAPS was provided by Calbiochem (Laeufelfingen, Switzerland). Plasmid carrying the SULT1A3 cDNA was a kind gift of Dr. Sakakibara, Department of Biochemistry, University of Miyazaki, Miyazaki, Miyazaki 889-2192, Japan.

Enantioselective Synthesis of Normetanephrines

The chemical protocols used for the synthesis of normetanephrines (compounds **8** and **9**, Scheme 1) are available as Supplementary Material, as is the procedure for determining enantiomeric excess and absolute configurations of intermediates **4** and **5**. All commercially available reagents and solvents (Fluka/Aldrich, Buchs, Switzerland and Acros, Wohlen, Switzerland) were used without further purification. For reactions requiring anhydrous conditions, dry solvents were obtained by filtration (Innovation Technology). Unless stated otherwise, experiments were carried out under an argon atmosphere. Reactions were monitored by thin-layer chromatography (Merck

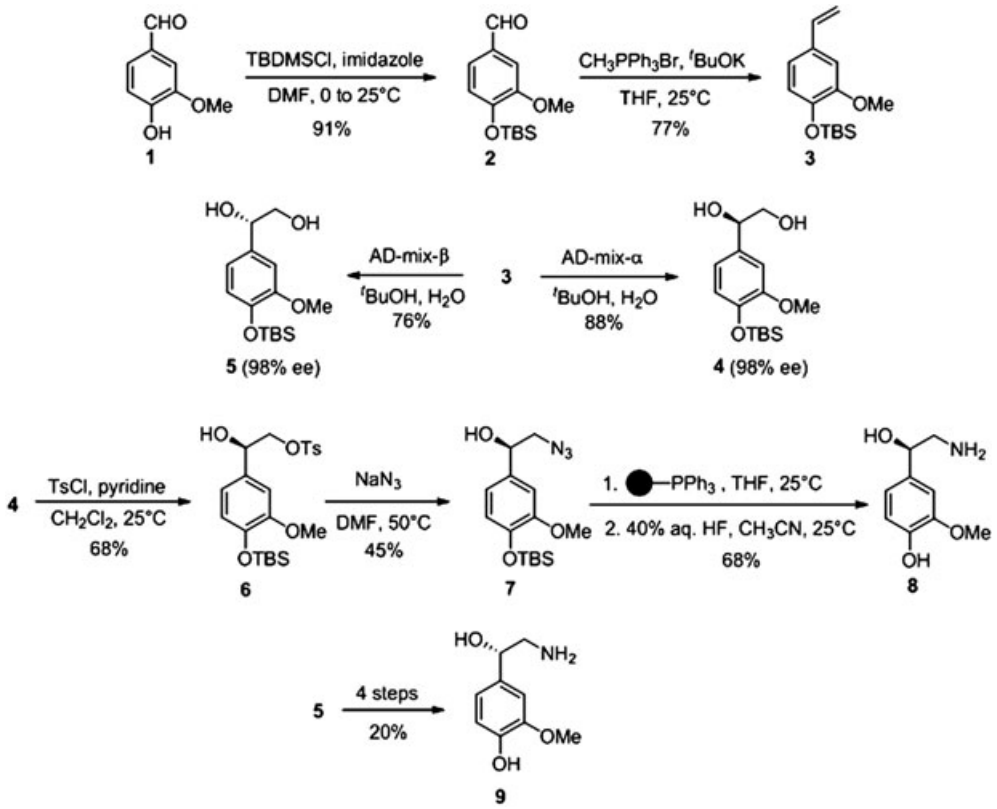

Scheme 1. The chemical synthesis of (1*R*)-normetanephrine (8) and (1*S*)-normetanephrine (9).

silica gel 60F254 plates), detection by UV light, $KMnO_4$, or Pancaldi reagents [$(NH_4)_6MoO_4$, $Ce(SO_4)$, H_2SO_4, H_2O]. Purifications were performed by flash chromatography on silica gel (Merck, Zoug, CH, N° 9385 silica gel 60, 240–400 mesh) and reverse phase HPLC. ^{1}H-NMR spectra: Bruker ARX-400, Bruker DPX-400 spectrometers at 400 MHz, and Bruker AVII-800 spectrometers at 800 MHz. Chemical shifts in ppm relative to the solvent's residual ^{1}H signal as internal reference were as follows: MeOD, 3.34 ppm; $CDCl_3$, 7.27 ppm; C_6D_6, 7.30 ppm. ^{1}H assignments were confirmed by 2D-COSY spectra. Multiplicity reflects apparent patterns. Coupling constants *J* are in Hz (b stands for broad). ^{13}C-NMR spectra: same instrument as above at 101 MHz. Reference values for solvents used as internal reference in ppm were as follows: MeOD, 49 ppm; $CDCl_3$; 77 ppm; C_6D_6, 128.5 ppm. Coupling constants *J* are in Hz. ^{13}C assignments were confirmed by 2D-HSQC spectra. IR spectra: Perkin-Elmer Paragon 1000 FTIR spectrometer. Mass spectra: MALDI-TOF spectrometer (Axima-CFR+, Kratos, Manchester, UK), ESI-Q spectrometer (Finnigan SSQ 710C, Thermoquest, UK), and HRMS-ESI spectrometer (Q-TOF Ultima spectrometer, Micromass, Manchester, UK).

The strategy envisaged for the enantioselective synthesis of (1*R*)-normetanephrine and (1*S*)-normetanephrine relied on asymmetric epoxidation or dihydroxylation to introduce the secondary alcohol of the side-chain with high enantioselectivity. Starting from vanillin, protection of the phenol as silyl ether followed by Wittig olefination of the aldehyde[15] delivered intermediate **3** in high yield (Scheme 1). Treatment with Jacobsen catalyst, in the presence of *meta*-chloroperbenzoic acid and *N*-methylmorpholine-*N*-oxide,[16–18] induced epoxidation of the olefin followed by subsequent opening of the oxirane by the *meta*-chlorobenzoic acid by-product. All our attempts to prevent opening of the epoxide during this step did not meet with success.

Gratifyingly, asymmetric dihydroxylation in the presence of AD-mix-α[19,20] delivered diol **4** in good yield and 98% enantiomeric excess (the enantiomeric excess and absolute configuration of the newly formed alcohol were determined from the ^{1}H-NMR spectra of the corresponding Mosher's esters[21,22] and supplementary data section). The use of AD-mix-α led to the formation of the other enantiomer **5** in 76% yield and 98% enantiomeric excess. Selective tosylation of the primary alcohol was a delicate transformation as migration of the *tert*-butyldimethylsilyl moiety from the phenol to the secondary alcohol was observed as side process. Portion-wise addition of tosyl chloride over 8 h was necessary to avoid this side reaction and delivered tosylate **6** in 68% yield. Nucleophilic displacement with an excess of sodium azide (10 eq) followed by Staudinger reduction of the resulting azide and cleavage of the silyl ether delivered (*R*)-normetanephrine **8** in high purity. The use of polymer bound triphenyl phosphine was necessary to avoid decomposition during the purification procedure. The same pathway was performed on diol **5** to afford (*S*)-normetanephrine **9** in 20% overall yield (four steps).

Preparation of Recombinant Sulfotransferase 1A3

The *SULT1A3* gene was cloned and expressed in *Escherichia coli* BL-21 strain (Promega, Walliselen, Switzerland) using the *pGEX-2TK* glutathione *S*-transferase gene fusion system and purified using glutathione Sepharose in conjunction with thrombin cleavage.[23]

Sulfotransferase Assay

(1*R*)-Normetanephrine, (1*S*)-normetanephrine, and rac-normetanephrine were incubated along with the sulfotransferase and PAPS, the universal sulfonyl group donor for SULT-catalyzed sulfonations. The reaction gives rise to a sulfated product and adenosine 3′,5′-diphosphate (PAP). The sulfotransferase assay was performed in 0.1 ml of 10 mM sodium phosphate buffer pH 6.8 containing 80 μM PAPS and (1*R*)-normetanephrine, (1*S*)-normetanephrine, or rac-normetanephrine at concentrations of 2.5, 5, 10, 20, 30, 40, 50, and 70 μM. The enzyme reaction was started by the addition of 300 ng of recombinant SULT1A3, and the incubation was stopped after 4 min at 37°C by adding one volume of mobile phase prior to injection on HPLC (50 μl). The rate of sulfonation was measured as a function of normetanephrine concentration, and the kinetic parameters were determined by fitting the Michaelis–Menten equation from which were derived the K_M and V_{max} constants. The reactions were performed in three separate experiments for each compound.

HPLC Method

The HPLC analyses were performed with an Alliance Instrument from Waters coupled with the corresponding UV detector set to 280 nm. Separation was carried out using a C18-reversed phase column (Macherey-Nagel, Basel, Switzerland). The mobile phase consisted of 217 mM sodium phosphate (NaH_2PO_4), 42.8 mM citric acid, and 546 μM octanesulfonic acid at pH 2.9 containing 2% acetonitrile. The flow rate was 0.9 ml/min; 25 μl of the incubation mixture was injected, and areas under the curve were determined for each substrate and metabolite (unconjugated and sulfoconjugated normetanephrine) and converted into concentrations on the basis of a calibration curve determined with synthetic free and sulfonated compounds. The reaction components had the following order of elution: PAPS (2.5 min), PAP (2.9 min), sulfonated normetanephrine (3.6 min), and free normetanephrine (9.8 min). K_M and V_{max} constants were determined from initial velocity measurements plotted versus different substrate concentrations using hyperbolic representations (GraphPad Prism Software, San Diego, CA, USA). K_M and V_{max} values were expressed as μM and pmol/min.

Docking Analysis by Molecular Modeling

The resolved structure of the human sulfotransferase SULT1A3 in complex with dopamine and PAP was retrieved from the PDB database (Id: 2A3R).[6] After deleting water molecules and adding hydrogen atoms, the structure was minimized keeping fixed the backbone atoms to conserve the experimental folding. The resulting structure was updated by manually modifying PAP into the PAPS cofactor whose atomic charges were attributed by PM6 semi-empirical calculations using MOPAC. The enzyme–cofactor complex was further minimized keeping fixed the atoms outside a 15-Å radius sphere around the modified cofactor and then used in the following docking analyses. The two enantiomers of normetanephrine were built in their protonated forms, and their conformational profile was investigated by a clustered MonteCarlo analysis as implemented in the VEGA suite of programs to produce 1000 minimized conformers.[24]

A sphere of 12.0 Å radius was defined around the bound dopamine, so encompassing the entire binding cavity. The resolution of the grid was $60 \times 50 \times 45$ points with a grid spacing of 0.450 Å. The dopamine molecule was then removed, and the lowest energy structures of the two enantiomers of normetanephrine were inserted in turn into the enzyme–cofactor complex within the 12.0-Å sphere using the AutoDock 4.0 software.[25] The ligands were then docked into this grid with the Lamarckian algorithm as implemented in AutoDock, and the flexible bonds of the ligand were left free to rotate. The genetic-based algorithm ran 20 simulations per substrate with 2,000,000 energy evaluations and a maximum number of generations of 27,000. The crossover rate was increased to 0.8, and the number of individuals in each population to 150. All other parameters were left at the AutoDock default settings. The obtained complexes were ranked considering both the AutoDock scores and the distance between the substrate's hydroxy group and cofactor. The chosen complexes were finally minimized keeping fixed the atoms outside a 15-Å radius sphere around the bound substrate and then used to recalculate docking scores and in the subsequent MD simulations.

Molecular Dynamics Simulations

The MD simulations involved SULT1A3 in complex with PAPS and the two normetanephrine enantiomers as generated by docking simulations. The complexes were firstly neutralized by adding nine Na^+ ions whose location was computed by the SODIUM software and then inserted into a 50-Å radius sphere of water molecules. After a preliminary minimization to optimize the relative position of solvent molecules, the systems underwent 5 nsec of all-atoms MD simulations with the following characteristics: (1) spherical boundary conditions were introduced to stabilize the simulation space; (2) Newton's equation was integrated using the r-RESPA method (every 4 fsec for long-range electrostatic forces, 2 fsec for short-range non-bonded forces, and 1 fsec for bonded forces); (3) the temperature was maintained at 300 ± 10 K by means of Langevin's algorithm; (4) Lennard–Jones interactions were calculated with a cutoff of 10 Å, and the pair list was updated every 20 iterations; (5) a frame was stored every 10 psec, yielding 500 frames; and (6) no constraints were applied to the systems.

The simulations were carried out in two phases: an initial period of heating from 0 to 300 K over 6000 iterations (6 psec, i.e., 1 K/20 iterations) and a monitored phase of simulation of 5 nsec. Only the frames memorized during this last phase were considered. All described minimizations were performed using the conjugate gradient algorithm. The calculations described here were carried out on a 16 CPU Tyan-VX50 system using Namd2.6 with the force field CHARMM and Gasteiger's atomic charges.[26]

RESULTS AND DISCUSSION

Enantioselective Synthesis of Normetanephrines

The challenges associated with the synthesis of optically pure normetanephrines relied on the high degree of functionalization of the aromatic core and the introduction of a chiral center on the lateral side chain, with high enantioselectivity. The use of vanillin as inexpensive starting material provided a good template for the sequential introduction of the different functional groups of normetanephrines, and Sharpless asymmetric dihydroxylation afforded both good yields and high enantioselectivities for the elaboration of the chiral secondary alcohol. The synthetic pathways disclosed herein represent reliable routes toward both enantiomers of normetanephrines with high optical purities, in seven steps and 11–13% overall yield from vanillin. The experimental procedures could be easily scaled up to produce meaningful quantities of these valuable biomarkers.

Incubations of Normetanephrines with Sulfotransferase 1A3

The maximum concentration of normetanephrine used to establish kinetic parameters was set at 50 μM because product inhibition was observed at higher normetanephrine concentrations (Fig. 2). The K_M values obtained for the production of the sulfoconjugated (1*R*)-normetanephrine, (1*S*)-normetanephrine, and rac-normetanephrine were similar: 1.90 ± 0.30, 1.82 ± 0.08, and 1.97 ± 0.66 μM, respectively ($P = 0.87$). The V_{max} values for the formation of the sulfoconjugates were 51.3 ± 1.5, 45.8 ± 2.8, and 46.8 ± 1.2 pmol/min, respectively ($P = 0.22$). SULT1A3 exhibited similar specificity constants toward the two enantiomers and the racemate of normetanephrine at 5.89, 5.26, and 5.38 min^{-1} ($P = 0.22$).

These experimental data suggest that the absolute configuration at C(1) bearing the hydroxyl group does not play a significant role in substrate affinity for SULT1A3 and that, at least for normetanephrine, the enzyme also binds and metabolizes the non-natural (1*S*)-enantiomer, in agreement with its broad tolerance to different substrates.[27] We are not aware of the existence of experimental results assessing the enantioselectivity of SULT1A3 toward norepinephrine and epinephrine.

Molecular Docking of the Sulfotransferase 1A3–Normetanephrine–3′-Phosphoadenosine-5′-phosphosulfate Complexes

Figure 3 compares the optimized poses of (1*S*)-normetanephrine (Fig. 3A) and (1*R*)-normetanephrine (Fig. 3B) in the catalytic cavity of the SULT1A3 enzyme. Except for the orientation of the hydroxyl group, a very similar arrangement of the two enantiomers is obvious in these figures. In other words, the two enantiomers adopt a comparable conformation in the optimized complexes.

Specifically, Figure 3 shows that the target *para*-hydroxyl group is very close to the PAPS cofactor and to the catalytic Lys106 and His108, a proximity conducive to the subsequent transfer of the SO_3 moiety.[28] The protonated amino group of both isomers is involved in ionic bonds with Asp86 and Glu89. For (1*R*)-normetanephrine, it also seems that Glu146 contributes to the negatively charged cage that surrounds and binds the protonated amino group. Furthermore, the two isomers share a similar network of apolar contacts that include π–π stacking of the substrate phenyl ring with Phe24, Phe81, Phe142, and Tyr240 plus hydrophobic interactions with Val84, Leu247, and Met248 (most of which not displayed in Figure 3 for reasons of clarity).

The only noteworthy difference between the two complexes lies in the orientation of the substrate's hydroxyl group. In the (1*S*)-normetanephrine complex (Fig. 3A), the hydroxyl group forms a strong intramolecular H-bond with the protonated amino group and seems to interact more weakly with Glu89. In the (1*R*)-normetanephrine complex (Fig. 3B), however, the hydroxyl group donates a H-bond to Glu146 and interacts weakly with a few other polar residues in its vicinity.

Another interesting difference between the two complexes lies in the position of some residues, most notably Asp86 and Glu89. It thus appears that while the two substrates adopt a comparable conformation in their respective complex, the enzymatic binding site alters and adapts the position of some of its key residues to maintain comparable weak bonds with functional groups close to C(1), the center of chirality in the substrate.

Various models have been proposed over more than a century to account for chiral recognition in protein–ligand complexes. The "Lock-and-Key Model" proposed in 1890 by Emil Fischer is far too limited as it does not account for the critical role played by ligand and target flexibility and mutual adaptability in increasing affinity.[29] An insightful model has been proposed to depict this process of mutual adaptability in biochemistry and pharmacology, namely the "induced-fit model".[29–32] In a metaphoric view, we may interpret our results by combining the "lock-and-key" and "induced fit" models such that the "lock" adapts itself to two enantiomeric "keys" of comparable conformation.

In summary, docking results indicate that the two enantiomers stabilize very similar patterns of interactions, thus suggesting a similar capacity to interact with SULT1A3. This is confirmed by the almost identical docking scores of the two complexes, namely −8.04 kcal/mol for (1*S*)-normetanephrine versus −8.11 for (1*R*)-normetanephrine. Further confirmation comes from the low value (0.91 Å) of the root-mean-square deviation (RMSD), a measure of the mean difference between the positions of the heteroatoms in the two docked enantiomers.

Molecular Dynamics of the Sulfotransferase 1A3–Normetanephrine–3′-Phosphoadenosine-5′-phosphosulfate Complexes

The computational methods used here are able to monitor conformation changes but in no way can they simulate the cleavage and formation of covalent bonds. This implies that they cannot monitor the course of an enzymatic reaction. Nevertheless, MD can assess the relative stability of docking complexes by simulating simultaneously conformational and translational movements.

With a view to further confirm the remarkable analogy between the poses of the two normetanephrine enantiomers in the SULT–normetanephrine–PAPS complexes, 5-nsec MD runs were performed that allow the stability of both complexes to be monitored for the duration of the simulations. A preliminary analysis concerned the folding stability of the

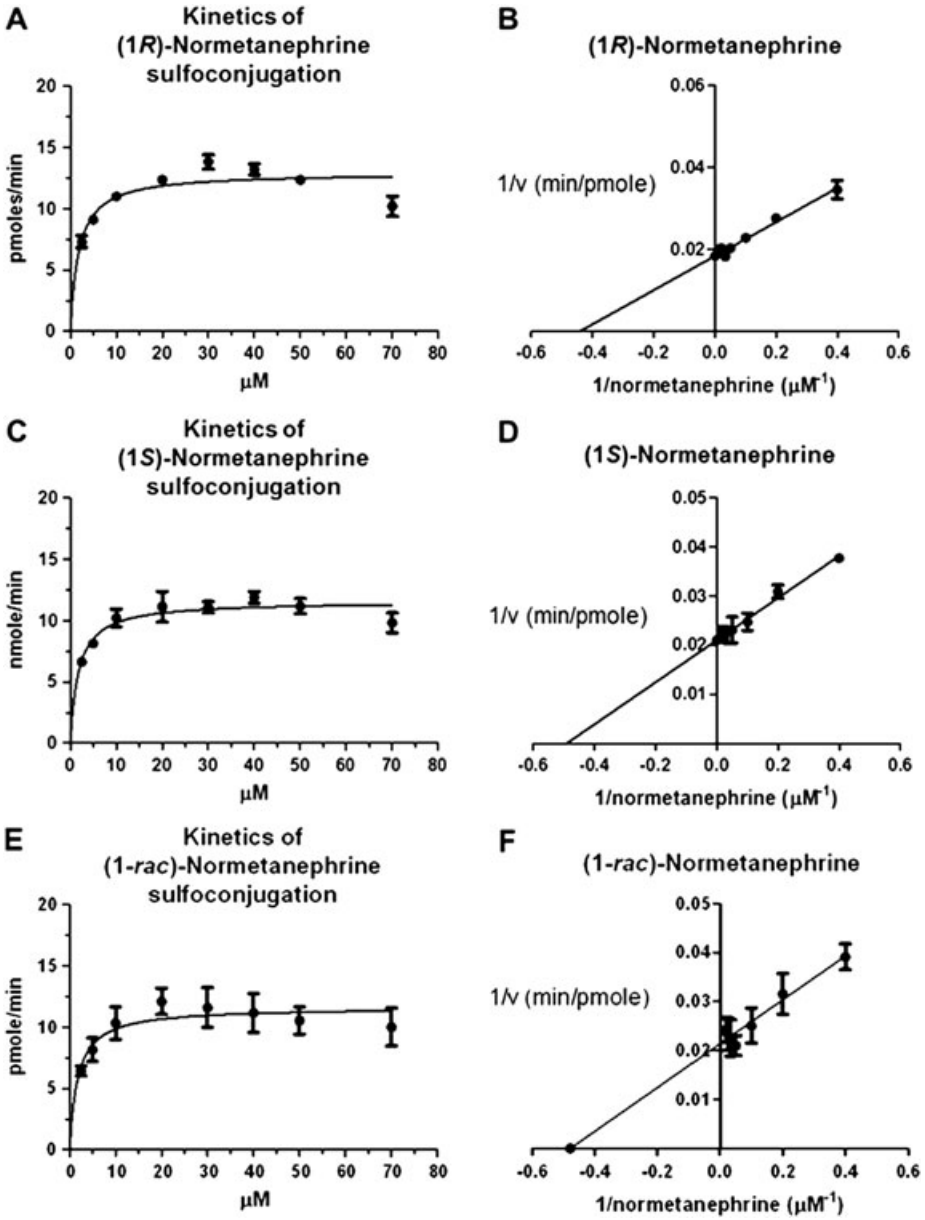

Fig. 2. Michaelis–Menten (A, C, and E) and Lineweaver Burk (B, D, and F) plots of the rate of sulfoconjugation of (1*R*)-normetanephrine, (1*S*)-normetanephrine, and rac-normetanephrine by recombinant human SULT1A3. The substrates were incubated at concentrations ranging from 5 to 70 μmol/l (*x*-axis). The products were quantified by HPLC. The reactions were performed in three separate experiments for each compound, and the error bars represent the standard deviations.

simulated protein as assessed by RMSD values (computed from backbone atoms only) and by the percentage of residues falling in the allowed regions of the Ramachandran plot. In the MD runs with either enantiomer, the enzyme protein showed a remarkable stability because the RMSD values remained constantly in a narrow range around 5 Å and the percentage of allowed residues did not vary significantly, remaining around 70% during the whole simulations (plots not shown). Such a folding stability suggests that the results described below are mainly due to the dynamic response of the enzyme and bound ligands and not to the random structural distortions.

The first major analysis concerned the stability of the cofactor binding as monitored by the distance between the Arg130 and the 3-phosphate group in PAPS. This ion-pair belongs to the network of ionic bonds (also involving Lys48, Lys106, Lys197, Arg257, and Lys258) that play a pivotal role in PAPS binding. Figure 4 clearly shows that PAPS remained stably bound within the catalytic cavity during both simulations. First, this result confirms the expected stability of the PAPS binding mode as resolved by X-ray analysis.[6] Furthermore, Figure 4 confirms the stability for the whole architecture of the catalytic site, thus indicating that the behavior of normetanephrine enantiomers truthfully mirrors the stability of the complexes and the absence of random distortions in the catalytic cavity.

The second major MD analysis concerned the stability for the computed poses of normetanephrine enantiomers as assessed by the length of the ionic bond between Asp86 and the protonated amino group in the substrate. Figure 5 shows that the length of this ionic bond fluctuated inside a narrow range (2.7 to 3.0 Å). Even more importantly, there was no detectable difference between the two enantiomers, a finding compatible with their similar enzyme affinity and productive stability in the cavity.

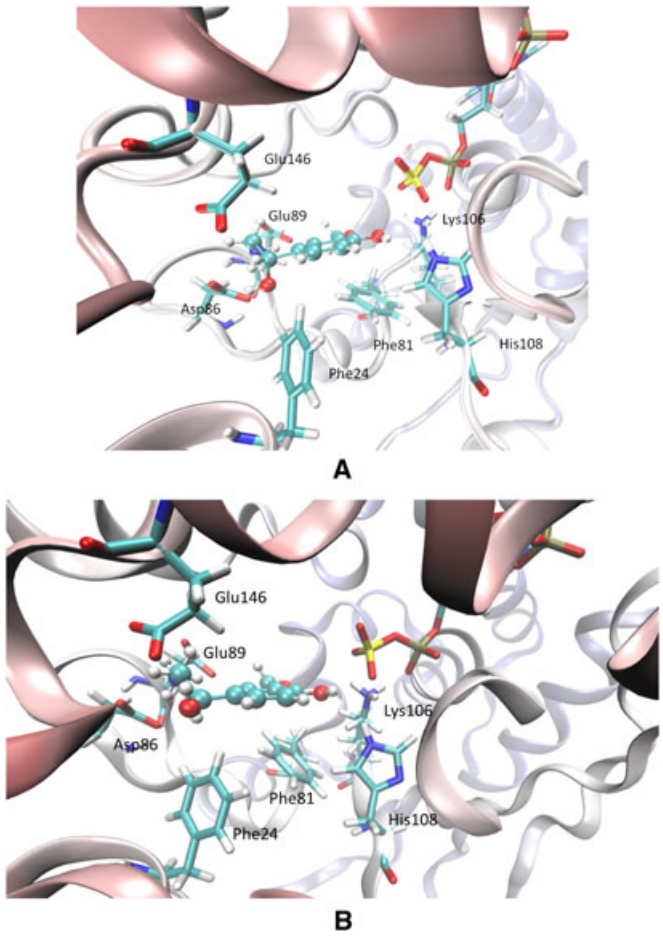

Fig. 3. Docking simulations showing the main interactions stabilizing the complexes between SULT1A3 and (1*S*)-normetanephrine (Figure 3A) or (1*R*)-normetanephrine (Figure 3B). See text for computational details.

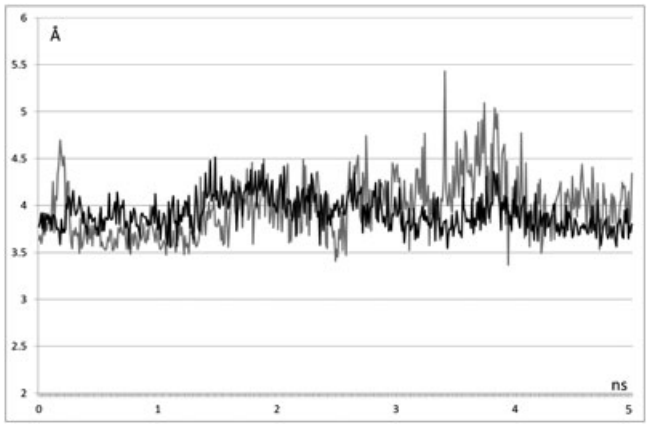

Fig. 4. Dynamic profile of the distance (in Angström) between Arg130 and the 3-phosphate group of PAPS in the SULT1A3–normetanephrine–PAPS complexes as obtained by molecular dynamics simulations. The gray line corresponds to the complex with (1*S*)-normetanephrine, and the black line to the complex with (1*R*)-normetanephrine. No meaningful difference exists between the two complexes, implying their similar stability. See text for computational details.

The enzyme kinetics investigations reported herein yielded an unexpected finding, namely the complete lack of substrate enantioselectivity of the SULT1A3-catalyzed sulfoconjugation of (1*R*)-normetanephrine and (1*S*)-normetanephrine. The

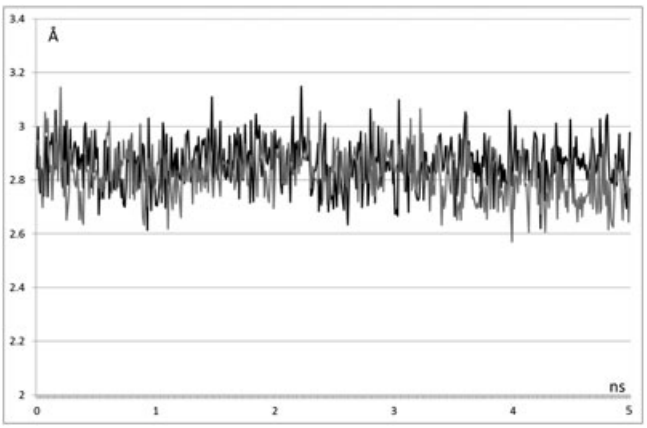

Fig. 5. Dynamic profile of the length of the ionic bond (in Angström) between the Asp86 and the protonated substrate amino group in the SULT1A3–normetanephrine–PAPS complexes as obtained by molecular dynamics simulations. The gray line corresponds to the complex with (1*S*)-normetanephrine, and the black line to the complex with (1*R*)-normetanephrine. No meaningful difference exists between the two complexes, implying their similar stability. See text for computational details.

results were obtained using the *ad hoc* synthetized normetanephrine enantiomers and expressed human SULT1A3.

Although this finding appears compatible with the broad substrate selectivity of SULT1A3,[27] it remains difficult to interpret. MM and MD simulations were therefore carried out in an attempt to understand the biomolecular mechanisms underlying this lack of enantioselectivity.

CONCLUSIONS

Taken together, docking computations and MD simulations have confirmed the substantial equivalence of the two computed binding modes in terms of both strength of stabilizing contacts and dynamic behavior during the simulation time. In other words, the computational results are compatible with and offer a molecular interpretation to the experimental finding that SULT1A3 conjugates both enantiomers of normetanephrine with undistinguishable affinity (K_M) and maximal rate of reaction (V_{max}).

ACKNOWLEDGMENTS

We thank Ms. Adeline Herren for her technical assistance. The authors are very grateful to Dr. Sakakibara for providing the plasmid encoding the gene SULT1A3.

CONFLICT OF INTEREST

The authors have declared that there is no conflict of interest.

LITERATURE CITED

1. Goldstein DS, Eisenhofer G, Kopin IJ. Sources and significance of plasma levels of catechols and their metabolites in humans. J Pharmacol Exp Ther 2003;305:800–811.
2. Testa B, Krämer SD. Metabolism. Volume 2: Conjugations, Consequences of Metabolism, Influencing Factors. Weinheim, Germany: Wiley-VCH, 2010;23–35.
3. Cappiello M, Giuliani L, Pacifici GM. Differential distribution of phenol and catechol sulphotransferases in human liver and intestinal mucosa. Pharmacology 1990;40:69–76.
4. Manger WM, Gifford RW. 1996 In clinical and experimental pheochromocytoma, 2nd ed. Cambridge: Blackwell Science.
5. Simonin J, Gerber-Lemaire S, Centeno C, Seghezzi C, Iglesias K, Abid K, Grouzmann E. Synthetic calibrators for the analysis of total

metanephrines in urine: revisiting the conditions of hydrolysis. Clin Chim Acta 2012;413:998–1003.

6. Lu JH, Li HT, Liu MC, Zhang JP, Li M, An XM, Chang WR. Crystal structure of human sulfotransferase SULT1A3 in complex with dopamine and 3′-phosphoadenosine 5′-phosphate. Biochem Biophys Res Commun 2005;335:417–423.
7. Dajani R, Hood AM, Coughtrie MW. A single amino acid, glu146, governs the substrate specificity of a human dopamine sulfotransferase, SULT1A3. Mol Pharmacol 1998;54:942–948.
8. Brix LA, Barnett AC, Duggleby RG, Leggett B, McManus ME. Analysis of the substrate specificity of human sulfotransferases SULT1A1 and SULT1A3: site-directed mutagenesis and kinetic studies. Biochemistry 1999;38:10474–10479.
9. Eaton E, Walle UK, Wilson HM, Aberg G, Walle T. Stereoselective sulphate conjugation of salbutamol by human lung and bronchial epithelial cells. Br J Clin Pharmacol 1996;41:201–206.
10. Hartman AP, Wilson AA, Wilson HM, Aberg G, Falany CN, Walle T. Enantioselective sulfation of β2-receptor agonists by the human intestine and the recombinant M-form phenolsulfotransferase. Chirality 1988;10:800–803.
11. Pesola GR, Walle, T. Stereoselective sulfate conjugation of isoproterenol in humans: comparison of hepatic, intestinal, and platelet activity. Chirality 1993;5:602–609.
12. Walle T, Walle UK. Stereoselective sulfate conjugation of 4-hydroxypropranolol and terbutaline by the human liver phenolsulfotransferases. Drug Metab Dispos 1992;20:333–336.
13. Walle UK, Pesola GR, Walle T. Stereoselective sulfate conjugation of salbutamol in humans: comparison of hepatic, intestinal and platelet activity. Br J Clin Pharmacol 1993;35:413–418.
14. Wilson AA, Wang J, Koch P, Walle T. Stereoselective sulphate conjugation of fenoterol by human phenolsulphotransferases. Xenobiotica 1997;27: 1147–1154.
15. Tilley SD, Francis MB. Tyrosine-selective protein alkylation using π-allylpalladium complexes. J Am Chem Soc 2006;128:1080–1081.
16. Jacobsen EN, Zhang W, Muci AR, Ecker JR, Deng LJ. Highly enantioselective epoxidation catalysts derived from 1,2-diaminocyclohexane. J Am Chem Soc 1991;113:7063–7064.
17. Palucki M, McCormick GJ, Jacobsen EN. Low temperature asymmetric epoxidation of unfunctionalized olefins catalyzed by (salen)Mn(III) complexes. Tetrahedron Lett 1995;36:5457–5460.
18. Zhang W, Loebach JL, Wilson SR, Jacobsen EN. Enantioselective epoxidation of unfunctionalized olefins catalyzed by salen manganese complexes. J Am Chem Soc 1990;112:2801–2803.
19. Kolb HC, Van Nieuwenhze MS, Sharpless KB. Catalytic asymmetric dihydroxylation. Chem Rev 1994;94:2483–2547.
20. Sharpless KB, Amberg W, Bennani YL, Crispino GA, Hartung J, Jeong KS, Kwong HL, Morikawa K, Wang ZM. The osmium-catalyzed asymmetric dihydroxylation: a new ligand class and a process improvement. J Org Chem 1992;57:2768–2771.
21. Dale JA, Dull DL, Mosher HS. α-Methoxy-α-trifluoromethylphenylacetic acid, a versatile reagent for the determination of enantiomeric composition of alcohols and amines. J Org Chem 1969;34:2543–2549.
22. Dale TA, Mosher HS. Nuclear magnetic resonance enantiomer reagents. Configurational correlations via nuclear magnetic resonance chemical shifts of diastereomeric mandelate, *O*-methylmandelate, and alpha-methoxy-alpha-trifluoromethylphenylacetate (MTPA) esters. J Am Chem Soc 1973;95:512–519.
23. Sakakibara Y, Takami Y, Nakayama T, Suiko M, Liu MC. Localization and functional analysis of the substrate specificity/catalytic domains of human M-form and P-form phenol sulfotransferases. J Biol Chem 1998;273:6242–6247.
24. Pedretti A, Villa L, Vistoli G. VEGA: a versatile program to convert, handle and visualize molecular structure on Windows-based PCs. J Mol Graph Model 2002;21:47–49.
25. Morris GM, Goodsell DS, Halliday RS, Huey R, Hart WE, Belew RK, Olson AJ. Automated docking using a Lamarckian genetic algorithm and empirical binding free energy function. J Comput Chem 1998;19:1639–1662.
26. Phillips JC, Braun R, Wang W, Gumbart J, Tajkhorshid E, Villa E, Chipot C, Skeel RD, Kalé L, Schulten K. Scalable molecular dynamics with NAMD. J Comput Chem 2005;16:1781–1802.
27. Bidwell LM, McManus ME, Gaedigk A, Kakuta Y, Negishi M, Pedersen L, Martin JL. Crystal structure of human catecholamine sulfotransferase. J Mol Biol 1999;293:521–530.
28. Testa B, Krämer SD. The biochemistry of drug metabolism—an introduction. Part 4: reactions of conjugation and their enzymes. Chem Biodivers 2008;5:2171–2336.
29. Koshland DE, Jr. The key-lock theory and the induced fit theory. Angew Chem Int Ed Engl 1994;33:2375–2378.
30. Johnson KA. Role of induced fit in enzyme specificity: a molecular forward/reverse switch. J Biol Chem 2008;283:26297–26301.
31. Post CB, Ray WJ Jr. Reexamination of induced fit as a determinant of substrate specificity in enzymatic reactions. Biochemistry 1995;34: 15881–15885.
32. Sotriffer CA. Accounting for induced-fit effects in docking: what is possible and what is not? Curr Top Med Chem 2011;11:179–191.